frontiers | Frontiers in Physics

TYPE Mini Review
PUBLISHED 17 October 2022
DOI 10.3389/fphy.2022.1057520

Check for updates

OPEN ACCESS

EDITED BY
Xiaoming Zhang,
Hebei University of Technology, China

REVIEWED BY
Guangqian Ding,
Chongqing University of Posts and Telecommunications, China
Mingmin Zhong,
Southwest University, China

*CORRESPONDENCE
Ying Yang,
20131184@cqnu.edu.cn

SPECIALTY SECTION
This article was submitted to Condensed Matter Physics, a section of the journal Frontiers in Physics

RECEIVED 29 September 2022
ACCEPTED 05 October 2022
PUBLISHED 17 October 2022

CITATION
Yang Y (2022), Phonoic nodal point in two dimensions: A mini-review.
Front. Phys. 10:1057520.
doi: 10.3389/fphy.2022.1057520

Phononic nodal point in two dimensions: A mini-review

Ying Yang*

College of Physics and Electronic Engineering, Chongqing Normal University, Chongqing, China

In recent decades, nodal point states in electronic systems have attracted significant interest in current research. Recently, the conceptual framework of nodal point states has been extended to bosonic systems, especially the phononic one. It is well known that the nodal point states may exist much more universally in materials other than topological electronic systems. Fortunately, a series of nodal point phonons are reported in three-dimensional realistic materials, and some are certified in experiments. However, to our knowledge, the study of phononic 2D nodal points is still relatively primitive. Hence, a highlight of research in the emerging area covering approximately the last two-three years is necessary. This mini-review will summary the recent advances in the phononic nodal point in two dimensions. Some typical examples, including graphene, CrI_3 monolayer, YGaI monolayer, TiB_4 monolayer, Ti_2P monolayer, and Cu_2Si monolayer, are concluded in this mini-review. The topological properties and possible applications of these material candidates are also summarized.

KEYWORDS

nodal point, Dirac point, Weyl point, phonons, 2D monolayer

Introduction

To this date, various topological quasiparticles in three-dimensional (3D) crystalline solids, such as nodal points [1–10], nodal lines [11–20], and nodal surfaces [21–27], have attracted widespread attention because of their unique physical properties and potential applications. As prominent examples, Dirac/Weyl nodal point materials refer to a class of solid materials that feature topology-/symmetry-protected band degeneracies around the Fermi level, such that the Dirac/Weyl equations can describe the low-energy fermionic excitations around the band crossings in high-energy region.

Recently, the searching of nodal point states has been extended to spinless phonon systems [28–45]. Phonons can be viewed as a perfect platform for realizing the nodal point states [46–58] due to their unique device applications and the advantages of whole frequency range observation. For example, Wang et al. [53] proposed a topological triangular Weyl complex composed of one double Weyl point and two single Weyl points in the phonon dispersion of three-dimensional α-SiO_2. Liu et al. [52] reported charge-four Weyl point phonons in three-dimensional realistic materials with space group numbers 195–199, and 207–214. Xie et al. [46] reported sixfold degenerate nodal-point phonons in three-dimensional materials, including C_3N_4, Sc_4C_3, Y_4Sb_3, and K_8Si_{46}. In 2021, Chen et al. [51] systematically investigated three-dimensional Dirac phonons in all space groups

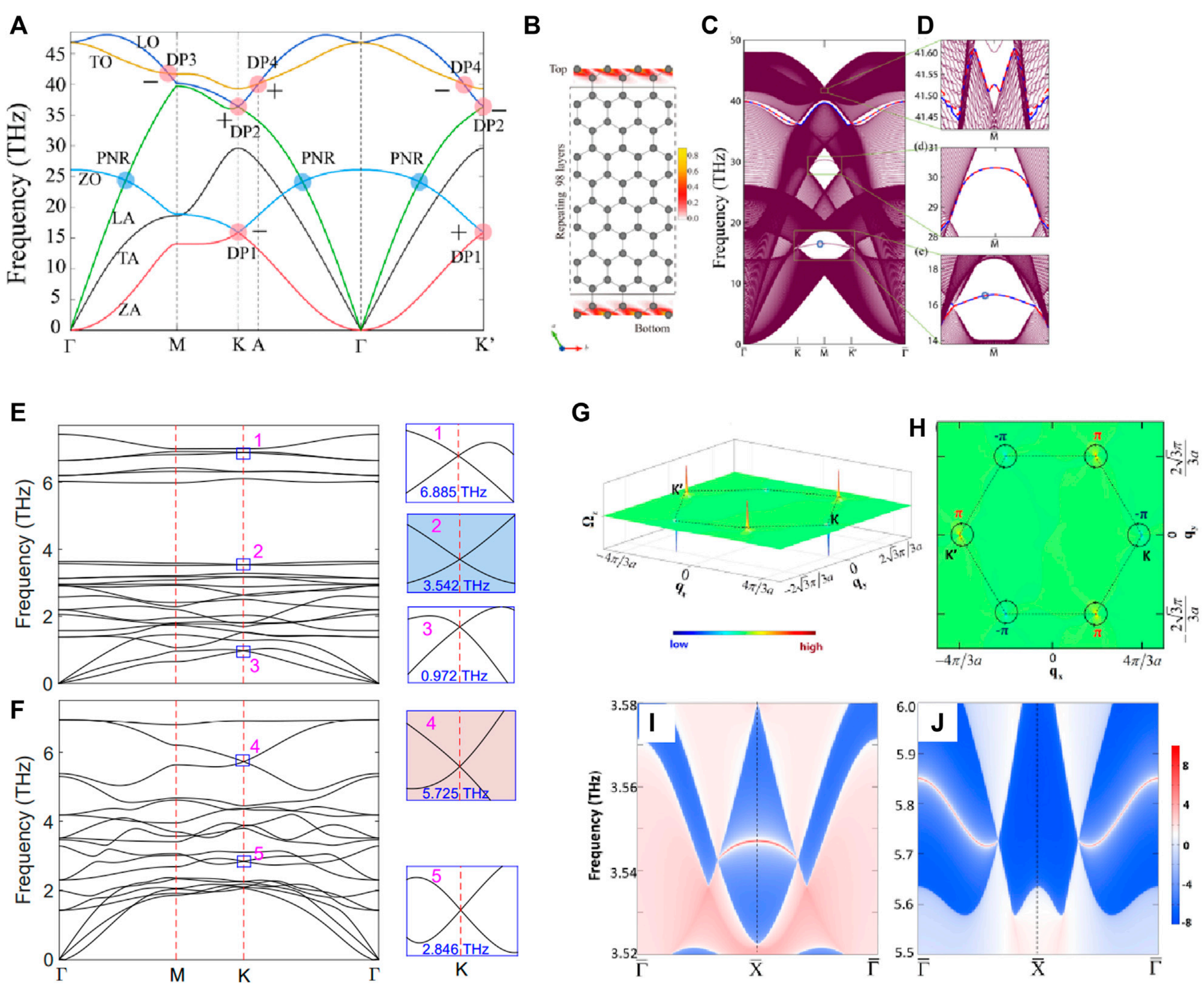

FIGURE 1
(A) phonon dispersion for graphene along Γ-M-K-A-Γ-K′ paths. The positions of DP1-DP4 and PNR are exhibited in **(A)**. **(B)** The ribbon model of graphene with a zigzag-edged boundary. **(C)** calculated phonon dispersion of the ribbon model and the edge states. **(D)** (from top to bottom) The enlarged figures of the edge states arise from the projections of DP3, PNR, and DP1 phonons, respectively. **(E)** and **(F)** the calculated phonon dispersions for the CrI_3 monolayer and YGaI monolayer, respectively. Boxes mark the positions of the Dirac points at the K high-symmetry point. The enlarged figures of the phonon bands in these boxes are also exhibited in **(E)** and **(F)**. **(G)** and **(H)** different views of Berry curvature distributions of CrI_3 with the Dirac frequency ω = 3.542 THz. **(I)** and **(J)** calculated edge states of semi-infinite nanoribbons for CrI_3 and YGaI with a zigzag-edged boundary. Reproduced from Refs. [60, 61] with permissions.

with inversion symmetry. Some realistic three-dimensional materials are also proposed in their work [22] to be candidate materials with Dirac point phonons. In 2022, Ding et al. [54] reported that three-dimensional $BaZnO_2$ has a type-III charge-two Weyl point phonon and double-helicoid phonon surface states. In the same year, Yang et al. [47] proposed the appearance of phononic nodal points with quadratic dispersion and multifold degeneracy in the three-dimensional Ta_3Sn. Experimentally, the double Weyl points in three-dimensional FeSi [56] were detected by inelastic x-ray scattering, which provided a strong driving force for the field.

However, to our knowledge, studying phononic nodal points in two dimensions is still relatively primitive. Only a handful of two-dimensional materials have been predicted to host phononic nodal points [59–61]. Hence, a highlight or summary of research in the emerging area of phononic nodal points in two dimensions covering approximately the last two-three year is highly desired. This mini-review highlights recent and vital developments in the phononic nodal points in two dimensions. The proposed phononic Dirac point and higher-order nodal point in two dimensions will be summarized, and some typical material candidates, including graphene, CrI_3 monolayer, YGaI monolayer, TiB_4 monolayer, Ti_2P monolayer,

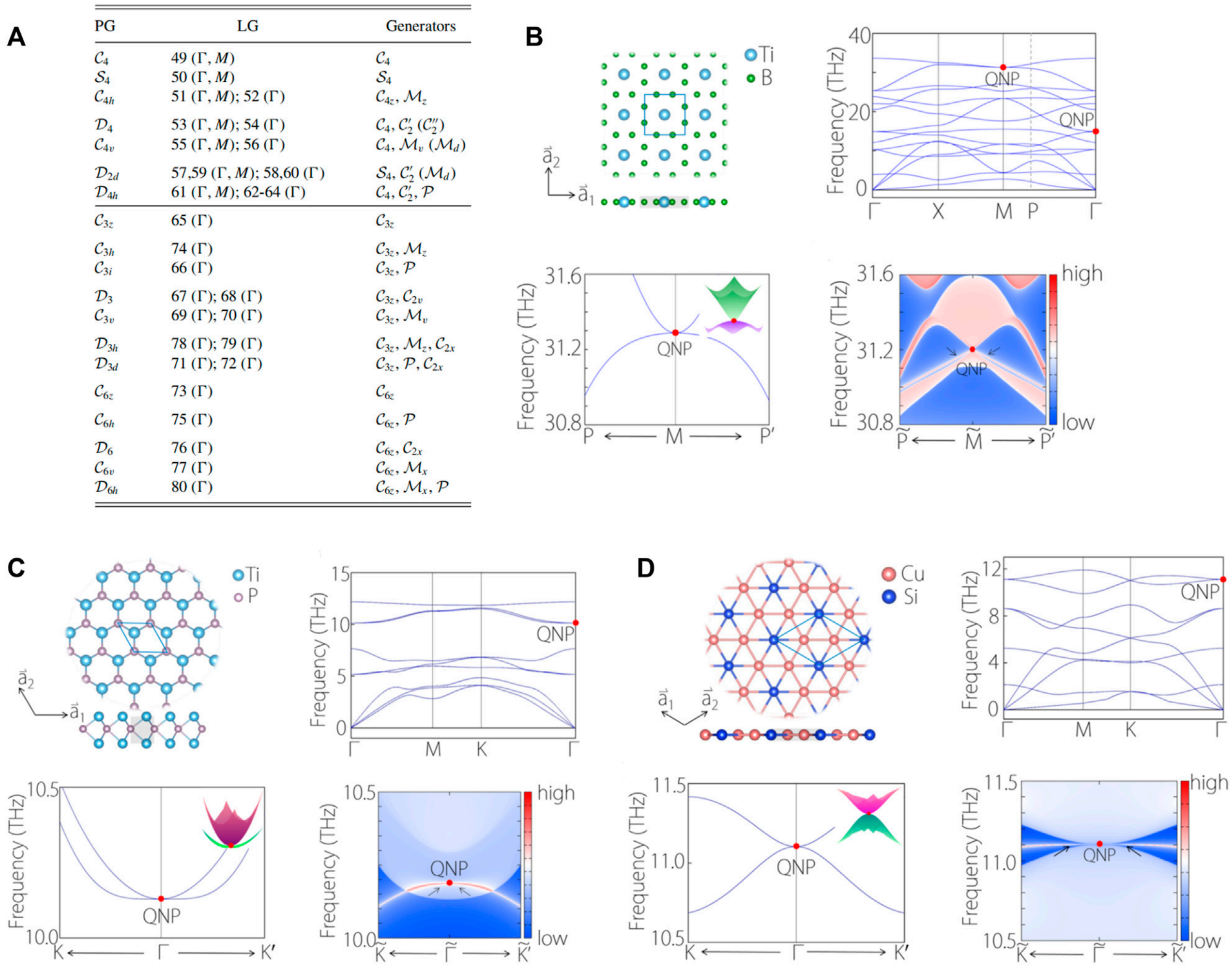

PG	LG	Generators
$\mathcal{C}_4$	49 (Γ, M)	$\mathcal{C}_4$
$\mathcal{S}_4$	50 (Γ, M)	$\mathcal{S}_4$
$\mathcal{C}_{4h}$	51 (Γ, M); 52 (Γ)	$\mathcal{C}_{4z}, \mathcal{M}_z$
$\mathcal{D}_4$	53 (Γ, M); 54 (Γ)	$\mathcal{C}_4, \mathcal{C}_2' (\mathcal{C}_2'')$
$\mathcal{C}_{4v}$	55 (Γ, M); 56 (Γ)	$\mathcal{C}_4, \mathcal{M}_v (\mathcal{M}_d)$
$\mathcal{D}_{2d}$	57,59 (Γ, M); 58,60 (Γ)	$\mathcal{S}_4, \mathcal{C}_2' (\mathcal{M}_d)$
$\mathcal{D}_{4h}$	61 (Γ, M); 62-64 (Γ)	$\mathcal{C}_4, \mathcal{C}_2', \mathcal{P}$
$\mathcal{C}_{3z}$	65 (Γ)	$\mathcal{C}_{3z}$
$\mathcal{C}_{3h}$	74 (Γ)	$\mathcal{C}_{3z}, \mathcal{M}_z$
$\mathcal{C}_{3i}$	66 (Γ)	$\mathcal{C}_{3z}, \mathcal{P}$
$\mathcal{D}_3$	67 (Γ); 68 (Γ)	$\mathcal{C}_{3z}, \mathcal{C}_{2v}$
$\mathcal{C}_{3v}$	69 (Γ); 70 (Γ)	$\mathcal{C}_{3z}, \mathcal{M}_v$
$\mathcal{D}_{3h}$	78 (Γ); 79 (Γ)	$\mathcal{C}_{3z}, \mathcal{M}_z, \mathcal{C}_{2x}$
$\mathcal{D}_{3d}$	71 (Γ); 72 (Γ)	$\mathcal{C}_{3z}, \mathcal{P}, \mathcal{C}_{2x}$
$\mathcal{C}_{6z}$	73 (Γ)	$\mathcal{C}_{6z}$
$\mathcal{C}_{6h}$	75 (Γ)	$\mathcal{C}_{6z}, \mathcal{P}$
$\mathcal{D}_6$	76 (Γ)	$\mathcal{C}_{6z}, \mathcal{C}_{2x}$
$\mathcal{C}_{6v}$	77 (Γ)	$\mathcal{C}_{6z}, \mathcal{M}_x$
$\mathcal{D}_{6h}$	80 (Γ)	$\mathcal{C}_{6z}, \mathcal{M}_x, \mathcal{P}$

FIGURE 2
(A) Lists of PG, LG, and Generators related to the phononic quadratic nodal points at high-symmetry points. **(B–D)** structural models, calculated phonon dispersions, enlarged phonon bands around the quadratic nodal points (QNPs), and the calculated edge states for TiB_4, Ti_2P, and Cu_2Si monolayers, respectively. Reproduced from Ref. [59] with permissions.

and Cu_2Si monolayer, are concluded in this mini-review. The author will also summarize these material candidates' related topological properties and possible applications in this mini-review.

Phononic dirac point in two dimensions

In 2020, Li *et al.* [61] proposed the topological phonons in graphene based on the first-principle calculation and symmetry analysis. The phonon dispersion of graphene is collected in Figure 1A, one finds that there exist four types of Dirac points (DPs), named DP1-DP4, respectively. From Figure 1A, the DP1 and DP2 locate at K and K′ high-symmetry points. The DP3 appears on Γ-M path and the DP4 appears on Γ-M surface path, respectively. Moreover, Li *et al.* [61] examined the topological signatures for these DPs by calculating the Berry phases of the DP1-DP4. The Berry phases of DP1-DP4 are highlighted by "+" and "-" for π and -π, respectively. Hence, DP1-DP4 appear in pairs and are topologically nontrivial.

Moreover, two phononic band crossing points around 24 THz are obvious along Γ-K and Γ-K′ paths (see Figure 1A). These two points are not isolated and should form a closed ring (i.e., phononic nodal ring (PNR)). Li et al. [61] also investigated the edge states for the two-dimensional graphene with the help of Green's function iteration method. The results of the edge states are collected in Figures 1C,D. The top figure of Figure 1D shows the edge states arising from the projections of DP3 phonons. The middle figure of Figure 1D shows the edge states arising from the projections of PNR phonons, and the bottom figure of Figure 1D shows the edge states arising from the projections of DP1 phonons. The appearance of the phononic nodal points is essential for graphenes, providing an excellent direction to investigate the interesting topological phonons in two dimensions. Moreover, the predictions of the phononic nodal point in two dimensions can pave a new way to study the related topological properties, such as destructive interference and quantum (anomalous/spin) Hall-like topological effects.

Interestingly, Jin, Wang, and Xu [60] proposed a method to generate Dirac phonon states with a quantized valley Berry phase in a two-dimensional hexagonal lattice. Using this method, they [60] proved that candidates with C_3 symmetry at corners of the hexagonal Brillouin zone could host robust valley Dirac phonons. With the help of first-principle calculations, the phonon dispersions of two typical examples, i.e., CrI_3 monolayer and YGaI monolayer, are calculated by Jin, Wang, and Xu [60]. The results are collected in Figures 1E, F, in which multiple Dirac points can be observed at K and K′ high-symmetry points. Note that the CrI_3 monolayer is a magnetic semiconductor with a Curie temperature of 42.8 K. In 2018, Jiang et al. [62] proposed that the magnetism of two-dimensional CrI_3 can be controlled by electrostatic doping. Hence, Jin, Wang, and Xu [60] paved a new way to study topological phonons in two-dimensional magnetic materials. Similar to the DP1 and DP2 located at K and K′ high-symmetry points in graphene, the Dirac point phonons appear at K and K′ in the CrI_3 monolayer and YGaI monolayer. As shown in Figures 1G,H, the quantized Berry phase of π and -π are verified at K′ and K valleys by calculating the Berry curvature distributions. The edge states for the CrI_3 monolayer are visibly terminated at the projections of the Dirac points at K and K'. Their work not only provides a broad application of topological phonons in two dimensions but also extends the aspect of valley physics.

Phononic higher-order nodal point in two dimensions

In 2022, Yu et al. [59] searched through 80-layer groups and found that the phononic higher-order nodal point can appear in two dimensions. The appearance of the phononic higher-order nodal points is protected by rotation (except the twofold one) and time-reversal symmetries. They also stated that the highest order of momentum in a two-dimensional system is the second order, named quadratic order. From Figure 2A, Yu et al. [59] pointed out that the phononic higher-order nodal points can appear in layer groups of 49–80. The high-symmetry points where the phononic higher-order nodal points appear, the PG, and the Generators are also exhibited in Figure 2A.

As shown in Figures 2B–D, they [59] proposed some two-dimensional material candidates, including TiB_4, Ti_2P, and Cu_2Si monolayers, hosting the quadratic nodal point phonons at high-symmetry points. The structural models and the calculated phonon dispersions for these three monolayers are collected in Figures 2B–D, respectively. A Z – valued topological invariant can show as $\mathcal{N} = \frac{1}{4\pi i}\oint_C Tr\sigma_z \mathcal{H}^{-1}(\boldsymbol{k})\nabla_{\boldsymbol{k}}\mathcal{H}(\boldsymbol{k}) \cdot d\boldsymbol{k}.$ Yu *et al.* [59] also stated that the two-dimensional quadratic nodal point could be characterized by an integer topological invariant, reflecting the appearance of the edge states. The visible edge states arising from the projections of the quadratic nodal points for these two-dimensional material candidates are collected in Figures 2B–D. Note that the edge states are very clean, benefitting the experimental detections.

Summary

In this mini-review, the author summarized the recent advances in the phononic nodal point in two dimensions covering approximately the last two-three years. Typical two-dimensional material candidates, such as the CrI_3 monolayer, YGaI monolayer, TiB_4 monolayer, Ti_2P monolayer, and Cu_2Si monolayer, are concluded in this mini-review. Their topological signatures and possible properties are also summarized. This mini-review is hoped to help study phononic nodal point phonons in two dimensions.

Author contributions

YY- investigations and writing.

Funding

YY is grateful for support from the key project of education planning supported by Chongqing municipal education commission (No. 2021-GX-013), the National Natural Science Foundation of China (No. 12175027), and the Basic Research and Frontier Exploration Project of Chongqing Municipality (cstc2018jcyjAX0820).

Conflict of interest

The author declares that the research was conducted in the absence of any commercial or financial relationships that could be construed as a potential conflict of interest.

Publisher's note

References

1 Young SM, Kane CL. Dirac semimetals in two dimensions. *Phys Rev Lett* (2015) 115(12):126803. doi:10.1103/physrevlett.115.126803

2 Liu ZK, Zhou B, Zhang Y, Wang ZJ, Weng HM, Prabhakaran D, et al. Discovery of a three-dimensional topological Dirac semimetal, Na3Bi. *Science* (2014) 343(6173):864–7. doi:10.1126/science.1245085

3 Armitage NP, Mele EJ, Vishwanath A. Weyl and Dirac semimetals in three-dimensional solids. *Rev Mod Phys* (2018) 90(1):015001. doi:10.1103/revmodphys.90.015001

4 Gibson QD, Schoop LM, Muechler L, Xie LS, Hirschberger M, Ong NP, et al. Three-dimensional Dirac semimetals: Design principles and predictions of new materials. *Phys Rev B* (2015) 91(20):205128. doi:10.1103/physrevb.91.205128

5 Wieder BJ, Kim Y, Rappe AM, Kane CL. Double Dirac semimetals in three dimensions. *Phys Rev Lett* (2016) 116(18):186402. doi:10.1103/physrevlett.116.186402

6 Yang BJ, Nagaosa N. Classification of stable three-dimensional Dirac semimetals with nontrivial topology. *Nat Commun* (2014) 5(1):4898–10. doi:10.1038/ncomms5898

7 Yan B, Felser C. Topological materials: Weyl semimetals. *Annu Rev Condens Matter Phys* (2017) 8:337–54. doi:10.1146/annurev-conmatphys-031016-025458

8 Lv BQ, Weng HM, Fu BB, Wang XP, Miao H, Ma J, et al. Experimental discovery of weyl semimetal TaAs. *Phys Rev X* (2015) 5(3):031013. doi:10.1103/physrevx.5.031013

9 Soluyanov AA, Gresch D, Wang Z, Wu Q, Troyer M, Dai X, et al. Type-ii weyl semimetals. *Nature* (2015) 527(7579):495–8. doi:10.1038/nature15768

10 Hosur P, Parameswaran SA, Vishwanath A. Charge transport in Weyl semimetals. *Phys Rev Lett* (2012) 108(4):046602. doi:10.1103/physrevlett.108.046602

11 Wang X, Ding G, Cheng Z, Surucu G, Wang XL, Yang T. Rich topological nodal line bulk states together with drum-head-like surface states in NaAlGe with anti-PbFCl type structure. *J Adv Res* (2020) 23:95–100. doi:10.1016/j.jare.2020.01.017

12 Wang X, Ding G, Khandy SA, Cheng Z, Zhang G, Wang XL, et al. Unique topological nodal line states and associated exceptional thermoelectric power factor platform in Nb 3 GeTe 6 monolayer and bulk. *Nanoscale* (2020) 12(32):16910–6. doi:10.1039/d0nr03704d

13 Wang X, Ding G, Cheng Z, Surucu G, Wang XL, Yang T. Novel topological nodal lines and exotic drum-head-like surface states in synthesized CsCl-type binary alloy TiOs. *J Adv Res* (2020) 22:137–44. doi:10.1016/j.jare.2019.12.001

14 Zhou F, Liu Y, Kuang M, Wang P, Wang J, Yang T, et al. Time-reversal-breaking Weyl nodal lines in two-dimensional A 3 C 2 (A= Ti, Zr, and Hf) intrinsically ferromagnetic materials with high Curie temperature. *Nanoscale* (2021) 13(17):8235–41. doi:10.1039/d1nr00139f

15 Zhou F, Cui C, Wang J, Kuang M, Yang T, Yu ZM, et al. Perovskite-type YRh3B with multiple types of nodal point and nodal line states. *Phys Rev B* (2021) 103(24):245126. doi:10.1103/physrevb.103.245126

16 Fang C, Weng H, Dai X, Fang Z. Topological nodal line semimetals. *Chin Phys B* (2016) 25(11):117106. doi:10.1088/1674-1056/25/11/117106

17 Yang SY, Yang H, Derunova E, Parkin SS, Yan B, Ali MN. Symmetry demanded topological nodal-line materials. *Adv Phys X* (2018) 3(1):1414631. doi:10.1080/23746149.2017.1414631

18 Hu J, Tang Z, Liu J, Liu X, Zhu Y, Graf D, et al. Evidence of topological nodal-line fermions in ZrSiSe and ZrSiTe. *Phys Rev Lett* (2016) 117(1):016602. doi:10.1103/physrevlett.117.016602

19 Bian G, Chang TR, Sankar R, Xu SY, Zheng H, Neupert T, et al. Topological nodal-line fermions in spin-orbit metal PbTaSe2. *Nat Commun* (2016) 7(1):10556–8. doi:10.1038/ncomms10556

20 Yu R, Fang Z, Dai X, Weng H. Topological nodal line semimetals predicted from first-principles calculations. *Front Phys (Beijing)* (2017) 12(3):127202–14. doi:10.1007/s11467-016-0630-1

21 Wu W, Liu Y, Li S, Zhong C, Yu ZM, Sheng XL, et al. Nodal surface semimetals: Theory and material realization. *Phys Rev B* (2018) 97(11):115125. doi:10.1103/physrevb.97.115125

22 Zhang X, Yu ZM, Zhu Z, Wu W, Wang SS, Sheng XL, et al. Nodal loop and nodal surface states in the Ti3Al family of materials. *Phys Rev B* (2018) 97(23):235150. doi:10.1103/physrevb.97.235150

23 Yang Y, Xia JP, Sun HX, Ge Y, Jia D, Yuan SQ, et al. Observation of a topological nodal surface and its surface-state arcs in an artificial acoustic crystal. *Nat Commun* (2019) 10(1):5185–7. doi:10.1038/s41467-019-13258-3

24 Qie Y, Liu J, Wang S, Sun Q, Jena P. Tetragonal C 24: A topological nodal-surface semimetal with potential as an anode material for sodium ion batteries. *J Mater Chem A Mater* (2019) 7(10):5733–9. doi:10.1039/c8ta11276b

25 Xiao M, Ye L, Qiu C, He H, Liu Z, Fan S. Experimental demonstration of acoustic semimetal with topologically charged nodal surface. *Sci Adv* (2020) 6(8):eaav2360. doi:10.1126/sciadv.aav2360

26 Yang T, Jin L, Liu Y, Zhang X, Wang X. Spin-polarized type-II nodal loop and nodal surface states in hexagonal compounds XTiO2 (X = Li, Na, K, Rb). *Phys Rev B* (2021) 103(23):235140. doi:10.1103/physrevb.103.235140

27 Xiao M, Fan S (2017). Topologically charged nodal surface. Available at: https://arxiv.org/abs/1709.02363

28 Liu Y, Chen X, Xu Y. Topological phononics: From fundamental models to real materials. *Adv Funct Mater* (2020) 30(8):1904784. doi:10.1002/adfm.201904784

29 Prodan E, Prodan C. Topological phonon modes and their role in dynamic instability of microtubules. *Phys Rev Lett* (2009) 103(24):248101. doi:10.1103/physrevlett.103.248101

30 Stenull O, Lubensky TC. Signatures of topological phonons in superisostatic lattices. *Phys Rev Lett* (2019) 122(24):248002. doi:10.1103/physrevlett.122.248002

31 Liu G, Jin Y, Chen Z, Xu H. Symmetry-enforced straight nodal-line phonons. *Phys Rev B* (2021) 104(2):024304. doi:10.1103/physrevb.104.024304

32 Zhou F, Zhang Z, Chen H, Kuang M, Yang T, Wang X. Hybrid-type nodal ring phonons and coexistence of higher-order quadratic nodal line phonons in an AgZr alloy. *Phys Rev B* (2021) 104(17):174108. doi:10.1103/physrevb.104.174108

33 Wang J, Yuan H, Liu Y, Zhou F, Wang X, Zhang G. Hourglass Weyl and Dirac nodal line phonons, and drumhead-like and torus phonon surface states in orthorhombic-type KCuS. *Phys Chem Chem Phys* (2022) 24(5):2752–7. doi:10.1039/d1cp05217a

34 Wang J, Yuan H, Yu ZM, Zhang Z, Wang X. Coexistence of symmetry-enforced phononic Dirac nodal-line net and three-nodal surfaces phonons in solid-state materials: Theory and materials realization. *Phys Rev Mater* (2021) 5(12):124203. doi:10.1103/physrevmaterials.5.124203

35 Zhou F, Chen H, Yu ZM, Zhang Z, Wang X. Realistic cesium fluogermanate: An ideal platform to realize the topologically nodal-box and nodal-chain phonons. *Phys Rev B* (2021) 104(21):214310. doi:10.1103/physrevb.104.214310

36 Ding G, Sun T, Wang X. Ideal nodal-net, nodal-chain, and nodal-cage phonons in some realistic materials. *Phys Chem Chem Phys* (2022) 24(18):11175–82. doi:10.1039/d2cp00731b

37 Liu QB, Fu HH, Wu R. Topological phononic nodal hexahedron net and nodal links in the high-pressure phase of the semiconductor CuCl. *Phys Rev B* (2021) 104(4):045409. doi:10.1103/physrevb.104.045409

38 Zheng B, Zhan F, Wu X, Wang R, Fan J. Hourglass phonons jointly protected by symmorphic and nonsymmorphic symmetries. *Phys Rev B* (2021) 104(6):L060301. doi:10.1103/physrevb.104.l060301

39 Zhang TT, Miao H, Wang Q, Lin JQ, Cao Y, Fabbris G, et al. Phononic helical nodal lines with PT protection in MoB2. *Phys Rev Lett* (2019) 123(24):245302. doi:10.1103/physrevlett.123.245302

40 Wang M, Wang Y, Yang Z, Fan J, Zheng B, Wang R, et al. Symmetry-enforced nodal cage phonons in Th2BC2. *Phys Rev B* (2022) 105(17):174309. doi:10.1103/physrevb.105.174309

41 Chen ZJ, Xie ZJ, Jin YJ, Liu G, Xu H. Hybrid nodal-ring phonons with hourglass dispersion in $AgAlO_2$. *Phys Rev Mater* (2022) 6(3):034202. doi:10.1103/physrevmaterials.6.034202

42 Xie C, Yuan H, Liu Y, Wang X, Zhang G. Three-nodal surface phonons in solid-state materials: Theory and material realization. *Phys Rev B* (2021) 104(13):134303. doi:10.1103/physrevb.104.134303

43 Liu Y, Zou N, Zhao S, Chen X, Xu Y, Duan W. Ubiquitous topological states of phonons in solids: Silicon as a model material. *Nano Lett* (2022) 22(5):2120–6. doi:10.1021/acs.nanolett.1c04299

44 Jin YJ, Chen ZJ, Xia BW, Zhao YJ, Wang R, Xu H. Ideal intersecting nodal-ring phonons in bcc C8. *Phys Rev B* (2018) 98(22):220103. doi:10.1103/physrevb.98.220103

45 Yang T, Gu Q, Wang P, Wu Z, Zhang Z. Phononic quadratic nodal lines of different types in Li2NaN. *Appl Phys Lett* (2022) 121(5):053102. doi:10.1063/5.0102217

46 Xie C, Liu Y, Zhang Z, Zhou F, Yang T, Kuang M, et al. Sixfold degenerate nodal-point phonons: Symmetry analysis and materials realization. *Phys Rev B* (2021) 104(4):045148. doi:10.1103/physrevb.104.045148

47 Yang T, Xie C, Chen H, Wang X, Zhang G. Phononic nodal points with quadratic dispersion and multifold degeneracy in the cubic compound Ta3Sn. *Phys Rev B* (2022) 105(9):094310. doi:10.1103/physrevb.105.094310

48 Sreeparvathy PC, Mondal C, Barman CK, Alam A. Coexistence of multifold and multidimensional topological phonons in KMgBO3. *Phys Rev B* (2022) 106(8): 085102. doi:10.1103/physrevb.106.085102

49 Li J, Xie Q, Ullah S, Li R, Ma H, Li D, et al. Coexistent three-component and two-component Weyl phonons in TiS, ZrSe, and HfTe. *Phys Rev B* (2018) 97(5): 054305. doi:10.1103/physrevb.97.054305

50 Wang J, Yuan H, Kuang M, Yang T, Yu ZM, Zhang Z, et al. Coexistence of zero-one-and two-dimensional degeneracy in tetragonal SnO2 phonons. *Phys Rev B* (2021) 104(4):L041107. doi:10.1103/physrevb.104.l041107

51 Chen ZJ, Wang R, Xia BW, Zheng BB, Jin YJ, Zhao YJ, et al. Three-dimensional Dirac phonons with inversion symmetry. *Phys Rev Lett* (2021) 126(18):185301. doi:10.1103/physrevlett.126.185301

52 Liu QB, Wang Z, Fu HH. Charge-four weyl phonons. *Phys Rev B* (2021) 103(16):L161303. doi:10.1103/physrevb.103.l161303

53 Wang R, Xia BW, Chen ZJ, Zheng BB, Zhao YJ, Xu H. Symmetry-protected topological triangular Weyl complex. *Phys Rev Lett* (2020) 124(10):105303. doi:10.1103/physrevlett.124.105303

54 Ding G, Zhou F, Zhang Z, Yu ZM, Wang X. Charge-two Weyl phonons with type-III dispersion. *Phys Rev B* (2022) 105(13):134303. doi:10.1103/physrevb.105.134303

55 Jin YJ, Chen ZJ, Xiao XL, Xu H. Tunable double Weyl phonons driven by chiral point group symmetry. *Phys Rev B* (2021) 103(10):104101. doi:10.1103/physrevb.103.104101

56 Miao H, Zhang TT, Wang L, Meyers D, Said AH, Wang YL, et al. Observation of double Weyl phonons in parity-breaking FeSi. *Phys Rev Lett* (2018) 121(3): 035302. doi:10.1103/physrevlett.121.035302

57 Zhang T, Song Z, Alexandradinata A, Weng H, Fang C, Lu L, et al. Double-Weyl phonons in transition-metal monosilicides. *Phys Rev Lett* (2018) 120(1): 016401. doi:10.1103/physrevlett.120.016401

58 Zhong M, Han Y, Wang J, Liu Y, Wang X, Zhang G. Material realization of double-Weyl phonons and phononic double-helicoid surface arcs with P213 space group. *Phys Rev Mater* (2022) 6(8):084201. doi:10.1103/physrevmaterials.6.084201

59 Yu WW, Liu Y, Meng W, Liu H, Gao J, Zhang X, et al. Phononic higher-order nodal point in two dimensions. *Phys Rev B* (2022) 105(3):035429. doi:10.1103/physrevb.105.035429

60 Jin Y, Wang R, Xu H. Recipe for Dirac phonon states with a quantized valley berry phase in two-dimensional hexagonal lattices. *Nano Lett* (2018) 18(12): 7755–60. doi:10.1021/acs.nanolett.8b03492

61 Li J, Wang L, Liu J, Li R, Zhang Z, Chen XQ. Topological phonons in graphene. *Phys Rev B* (2020) 101(8):081403. doi:10.1103/physrevb.101.081403

62 Jiang S, Li L, Wang Z, Mak KF, Shan J. Controlling magnetism in 2D CrI_3 by electrostatic doping. *Nat Nanotechnol* (2018) 13(7):549–53. doi:10.1038/s41565-018-0135-x